

## Diphenylethoxy-substituted metal-free and metallophthalocyanines as potential photosensitizer for photodynamic therapy: synthesis and photophysical and photochemical properties

Yusuf YILMAZ<sup>1</sup>, Ali ERDOĞMUŞ<sup>2,\*</sup>, Muhammet Kasım ŞENER<sup>2</sup>

<sup>1</sup>Department of Chemistry, Gaziantep University, Gaziantep, Turkey

<sup>2</sup>Department of Chemistry, Yıldız Technical University, Davutpaşa, İstanbul, Turkey

Received: 12.06.2014 • Accepted: 23.07.2014 • Published Online: 24.11.2014 • Printed: 22.12.2014

**Abstract:** The synthesis of a 4-(2,2-diphenylethoxy)phthalonitrile (**1**) and its organosoluble free base (**2**), zinc(II) (**3**), nickel(II) (**4**), and cobalt(II) (**5**) phthalocyanine derivatives is presented in this work. The novel complexes were characterized by elemental analyses and spectral data such as infrared, nuclear magnetic resonance, ultraviolet visible, and mass data. General tendencies were described for photophysics (fluorescence) and photochemistry (photodegradation and singlet oxygen quantum yields) of the free base and zinc(II) phthalocyanine derivatives in dimethylformamide. The quantum yield values of fluorescence ( $\Phi_F$ ), singlet oxygen formation ( $\Phi_\Delta$ ), and photodegradation ( $\Phi_d$ ) for the zinc phthalocyanine were found to be 0.37, 0.48, and  $9.12 \times 10^{-4}$ , respectively. The photophysicochemical properties of the phthalocyanines (**2** and **3**) clearly reveal that these phthalocyanines could be used in singlet oxygen applications such as photodynamic therapy.

**Key words:** Phthalocyanine, singlet oxygen, photodynamic therapy, fluorescence quantum yield

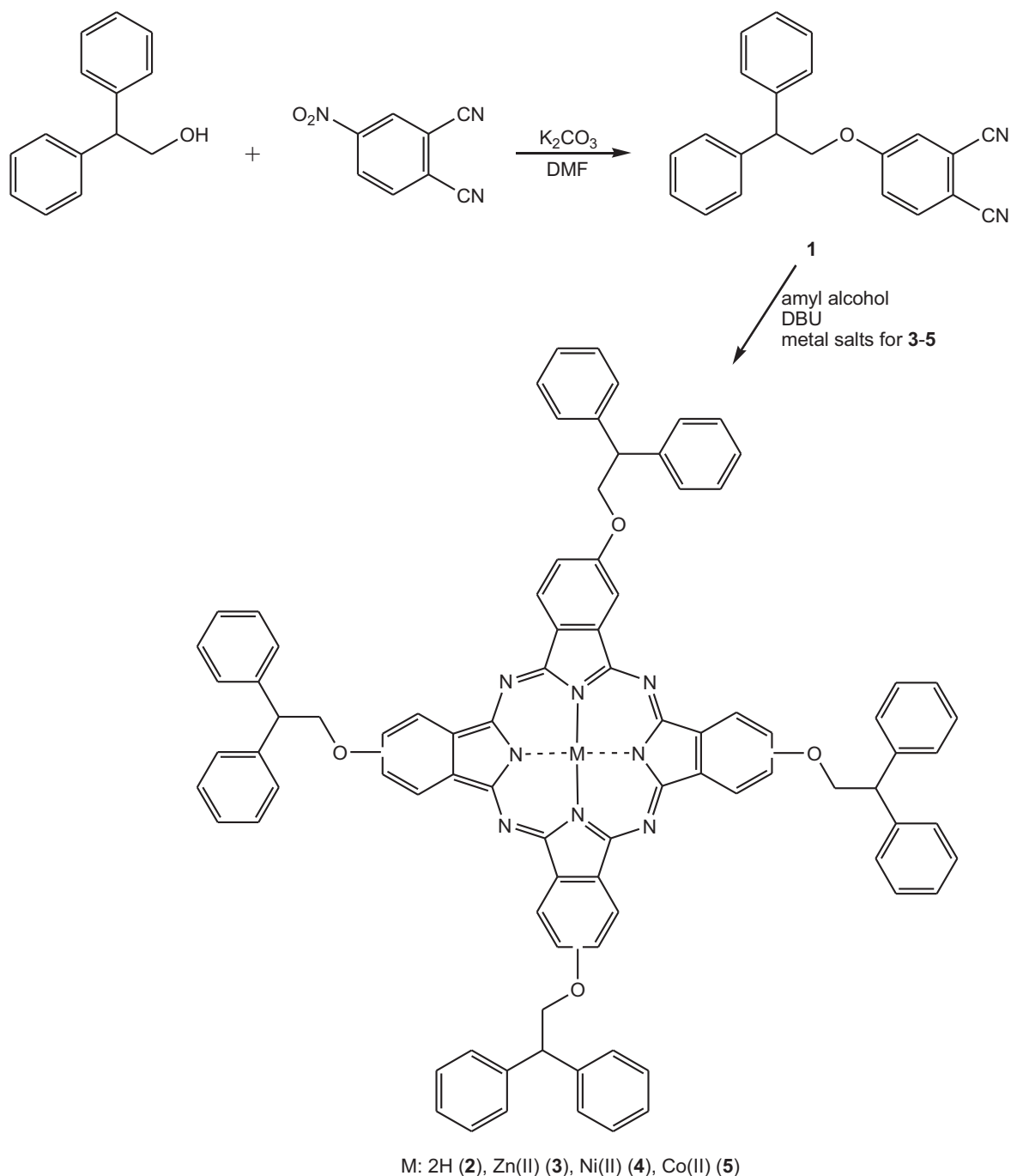
### 1. Introduction

Porphyrin-derived compounds are well known among the most widely studied of all macrocyclic systems.<sup>1–3</sup> Phthalocyanines (Pcs) are among the members of the macrocyclic systems that have attracted attention due to their potential use in photodynamic therapy (PDT), energy transfer, electrophotography, optical data collection, gas sensors, liquid crystals, laser technology, one-dimensional metals, and dyes and pigments.<sup>4</sup> Technological applications of unsubstituted Pcs are limited due to their insolubility in some organic solvents and aqua media. Pcs have an expanded  $\pi$ -conjugated electron system that allows  $\pi$  stacking (aggregation) between planar macrocycles, ensuring that the distance between macrocycles is small. Inserting substituents into the peripheral positions of the macrocycles enhances their solubility since these groups increase the space between the stacked Pc core and activate their solvation. Peripheral substitution<sup>5</sup> enables Pc products to be soluble in apolar solvents. Pcs have substituents whose carboxyl or quaternary ammonium moiety enhances solubility in a wide pH range of aqueous solutions.<sup>6–9</sup>

One of the most important usage of Pcs is as photosensitizers for PDT in cancer treatment in medicinal fields.<sup>10</sup> This application is rooted in the light excitation of a photosensitizer, which causes local oxidative harm within the cells by generation of extremely reactive oxygen species.<sup>11</sup> For PDT, it is highly important that Pcs

\*Correspondence: [erdogmusali@hotmail.com](mailto:erdogmusali@hotmail.com)

show high absorption coefficients in the visible region of the spectrum, mostly in the phototherapeutic window (600–800 nm), and a long lifetime of triplet excited state in order to generate reactive singlet oxygen species  $O_2(^1\Delta_g)$  proficiently.<sup>12</sup> The photophysical properties of Pc sensitizers are powerfully influenced by the central metal ion nature. The zinc(II) Pc complexes demonstrate attractive photophysical properties



**Scheme.** Synthetic scheme of tetra (2,2-diphenylethoxy) substituted free base (**2**), zinc (**3**), nickel (**4**), and cobalt (**5**) phthalocyanine derivatives.

and particularly high singlet oxygen generation, which are very significant for PDT of cancer.<sup>13–17</sup> Thus, many scientists have grown interested in Pc chemistry study of the synthesis and photophysical properties of Pcs in recent years.<sup>14,18–22</sup>

In the current study, the syntheses and characterization of the novel free base and metallophthalocyanine complexes having a diphenylethoxy group on each benzo group are described (Scheme). Photophysical (fluorescence quantum, singlet oxygen, and photodegradation quantum yields) characteristics of zinc(II) and free base Pc derivatives are investigated as well.

## 2. Results and discussion

### 2.1. Synthesis and characterization

The Scheme shows the synthetic route of novel peripherally tetra-substituted Pcs (**2–5**) involving the nucleophilic aromatic substitution of 4-nitrophthalonitrile with 2,2-diphenylethanol. Base-catalyzed nucleophilic aromatic substitution of 4-nitrophthalonitrile resulted in 4-(2,2-diphenylethoxy) phthalonitrile (**1**). The reaction was carried out at 45 °C in dry dimethylformamide with K<sub>2</sub>CO<sub>3</sub>. This reaction has been used in the preparation of a variety of ether or thioether substituted phthalonitriles.<sup>23</sup>

Reaction of the substituted phthalonitrile (**1**) with metal salts in the presence of metal salts in pentanol through a metal-assisted cyclotetramerization process gives the peripherally tetra-substituted Pcs (**3–5**). On the other hand, metal-free Pc derivative **2** was synthesized in amyl alcohol using DBU as a catalyst. The Pcs were isolated by column chromatography on silica gel. Because the Pcs have single substituent on each benzo group, they are all a mixture of 4 constitutional isomers. The novel metallophthalocyanines are effortlessly soluble in known solvents, like dimethyl sulfoxide (DMSO), dimethylformamide, toluene, chloroform (CHCl<sub>3</sub>), tetrahydrofuran (THF), and acetone, and are slightly soluble in dichloromethane (DCM).

The structures of the new compounds were verified by elemental analysis together with FT-IR, <sup>1</sup>H NMR, UV-Vis, and MS spectroscopic techniques. The FT-IR spectrum of **1** indicated the presence of aromatic, aliphatic, C≡N, and C=C groups by the intense stretching bands at 3081–3028, 2970–2894, 2228, and 1592 cm<sup>-1</sup>, respectively. The <sup>1</sup>H NMR spectrum of **1** exhibited the aromatic protons, integrating for a total of 13, at 7.71 ppm as a doublet for 1H, at 7.36 ppm as a triplet for 4H, at 7.28 ppm as a triplet for 7H, and at 7.19 ppm as a double doublet for 1H. Additionally, CH and CH<sub>2</sub> protons of **1** were observed at 4.56 ppm as a doublet and at 1.59 ppm as a triplet, which integrated for 3 protons. The FT-IR spectra of the Pcs confirmed the formation of the macrocycles, due to disappearance of the sharp triple bond signal seen for **1** at 2228 cm<sup>-1</sup>.<sup>24,25</sup>

The spectra obtained from <sup>1</sup>H NMR show that the Pcs were effectively purified. The protons of the rings are observed to lie in their individual regions. The <sup>1</sup>H NMR spectra of the peripherally tetra-substituted Pcs are just about the same as those of the initial compound, except for extension and small shifts of the peaks. It is expected that the broadening is due to both chemical exchange caused by an aggregation-disaggregation equilibrium in CDCl<sub>3</sub> and the presence of mixtures of 4 positional isomers with chemical shifts, which are expected to differ slightly from each other.<sup>26</sup> The signals for the aromatic protons of the substituents, Pc, and the periphery of the ligands of **2–4** appear to lie between 7.74 and 7.25, 7.73 and 7.07, and 7.64 and 7.20 ppm, respectively. In each case the integrated stringency is seen with the presence of 36 protons. Doublet peaks are observed for the 8 CH<sub>2</sub> protons at 4.67, 4.61, and 5.06 ppm and triplet peaks for the 4 CH protons at 1.75, 1.29, and 1.33 ppm for **2**, **3**, and **4**, respectively. The inner N-H proton signals of metal-free Pc in CHCl<sub>3</sub> were not observed, probably due to broadening related to tautomerism or aggregation effects.<sup>27</sup> In the MALDI-TOF

mass spectrum, we observed  $[M+H]^+$  peaks at 1300.7, 1363.8, and 1357.5 (see Figure 1 as an example for **5**) for **2**, **3**, and **5**, respectively. We also observed a  $[M]^+$  peak at 1355.5 for **3**. The elemental analysis results were also consistent with the desired structures of **1–5**. All of the spectral and elemental analysis results confirm that the target structures were successfully synthesized.

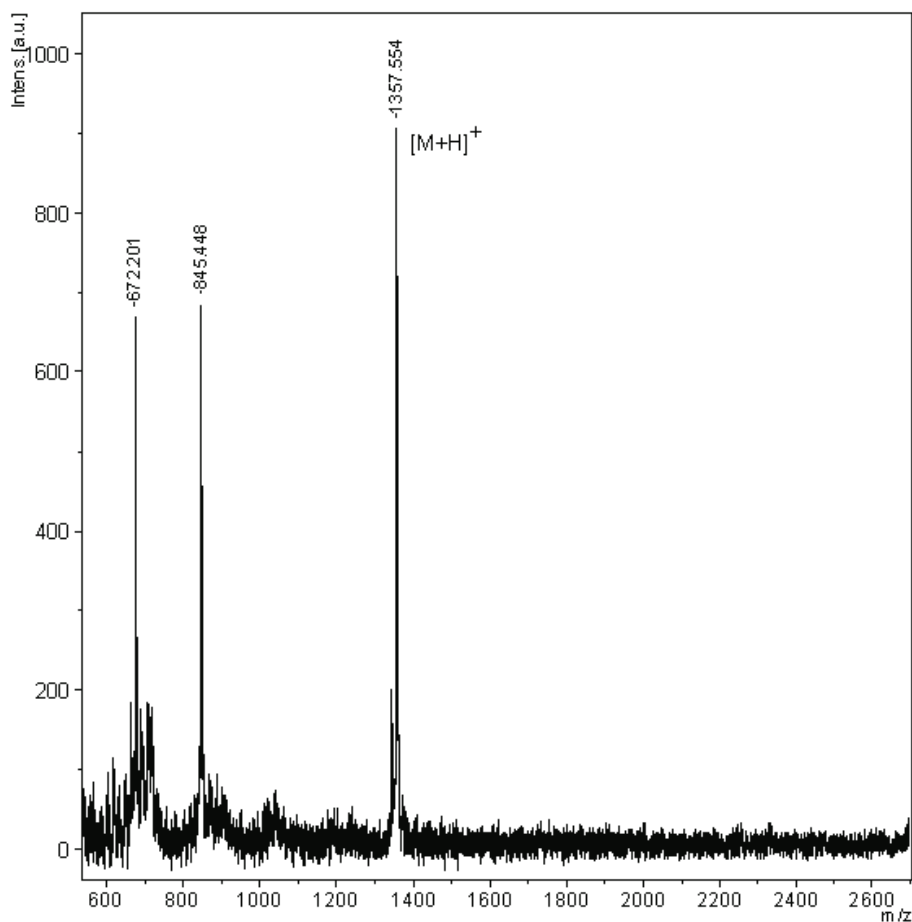
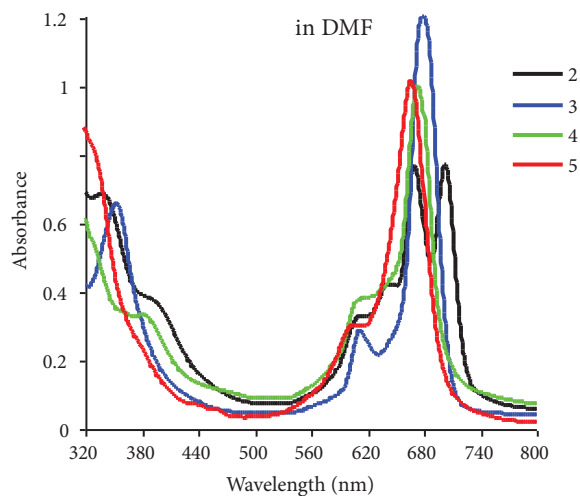


Figure 1. MALDI-TOF MS data for **5**.

## 2.2. Ground state electronic absorption and fluorescence spectra

UV-Vis electronic spectra are especially practical for identifying the structure of Pcs. Generally, for Pc complexes, UV-Vis spectra show typical electronic spectra with 2 strong absorption bands known as Q and Soret bands (B).<sup>28</sup> The electronic absorption spectra of the synthesized complexes (**2–5**) showed monomeric behavior provided by a single (narrow) Q band, typical of metallated Pcs in DMF at concentrations of about  $1.2 \times 10^{-5}$ . UV-Vis spectra of Pc complexes **2**, **3**, **4**, and **5** are shown in Figure 2. In the UV-Vis spectrum of free base Pc (**2**), the characteristic split Q band was observed at 670 and 703 nm in DMF, which can be attributed to  $a_{1u} \rightarrow e_g$  transition.<sup>29</sup> A typical spectrum of the metal-free Pc (**2**) showed a Soret band at 352 nm in DMF (Figure 2). The UV-Vis absorption spectra of metallophthalocyanines **3**, **4**, and **5** in DMF were observed with intense Q absorption at 679, 675, and 667 nm, respectively. In addition, the intense B band absorptions were observed at 352 nm for **3** and 379 nm for **4** in DMF. B band absorption was not observed for **5** in DMF (Figure 2). The

Q band of the zinc Pc (**3**) was red-shifted when compared to the corresponding other synthesized cobalt and nickel Pcs (**4** and **5**) in DMF on account of the central metal effect in the Pc core. The absorption maxima of the Q band for the zinc Pcs are nearly 20 nm longer than those of other metal Pcs, such as Mg, Al, Zn, and Ga, which are more suitable for PDT applications.



**Figure 2.** Absorption spectra of **2–5** in DMF at concentrations of  $\sim 1.2 \times 10^{-5}$ .

Aggregation tendency is typically defined as a coplanar relationship of rings succeeding from monomer to dimer and higher classified complexes. It can be affected by the temperature, kind of the solvent, concentration of solutions, structure and nature of substituents, and type of metal ions in the Pc core. In this work, we investigated the aggregation properties of Pc complexes **2–5** in DMF. For whole complexes synthesized, as the concentration was increased, the intensity of absorption of the Q band also increased and there were no new bands (blue or red region) observed in DMF. The Beer–Lambert law was followed for all of the Pcs in different concentrations ranging from  $2 \times 10^{-6}$  to  $12 \times 10^{-6}$  mol dm $^{-3}$  (see Figure 3 as an examples for complexes **3** (Figure 3a) and **4** (Figure 3b)).

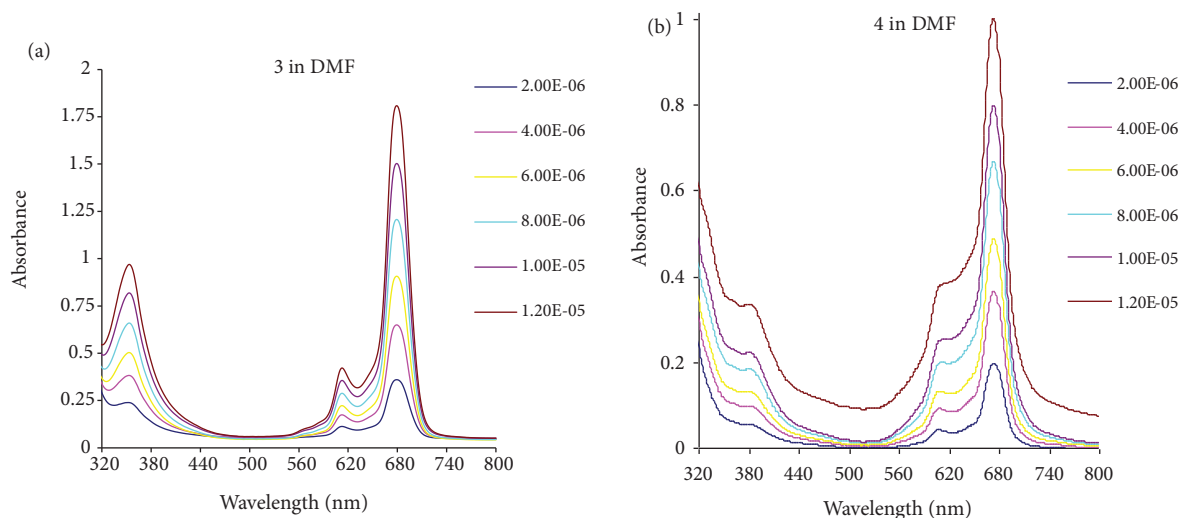


**Figure 3.** Absorption spectral changes of **3** (a) and **4** (b) in DMF at different concentrations:  $2 \times 10^{-6}$  (A),  $4 \times 10^{-6}$  (B),  $6 \times 10^{-6}$  (C),  $8 \times 10^{-6}$  (D),  $10 \times 10^{-6}$  (E),  $12 \times 10^{-6}$  mol dm $^{-3}$ .

The fluorescence properties of the free base (**2**) and zinc (**3**) Pc complexes were studied in DMF. Figure 4 shows the fluorescence emission, excitation, and absorption spectra for compounds **2** (Figure 4a) and **3** (Figure 4b) as examples in DMF. Fluorescence emission intensities were observed at 715 nm for **2** and 694 nm for **3**. The shapes of the excitation spectra ( $\lambda_{Ex} = 705$  nm for **2** and 685 nm for **3**) of synthesized Pc complexes were conformable to their absorption spectra. This closeness of the wavelength of the Q band absorption to the Q band maxima of the excitation spectrum for Pcs suggests that the nuclear configurations of the ground and excited states are similar and are not affected by excitation. Stokes shifts are observed at 12 nm for **2** and 14 nm for **3** in DMF. Because of the paramagnetic nature of the metals, the nickel<sup>30</sup> (**4**) and cobalt<sup>31</sup> (**5**) Pcs did not display fluorescence properties in DMF.

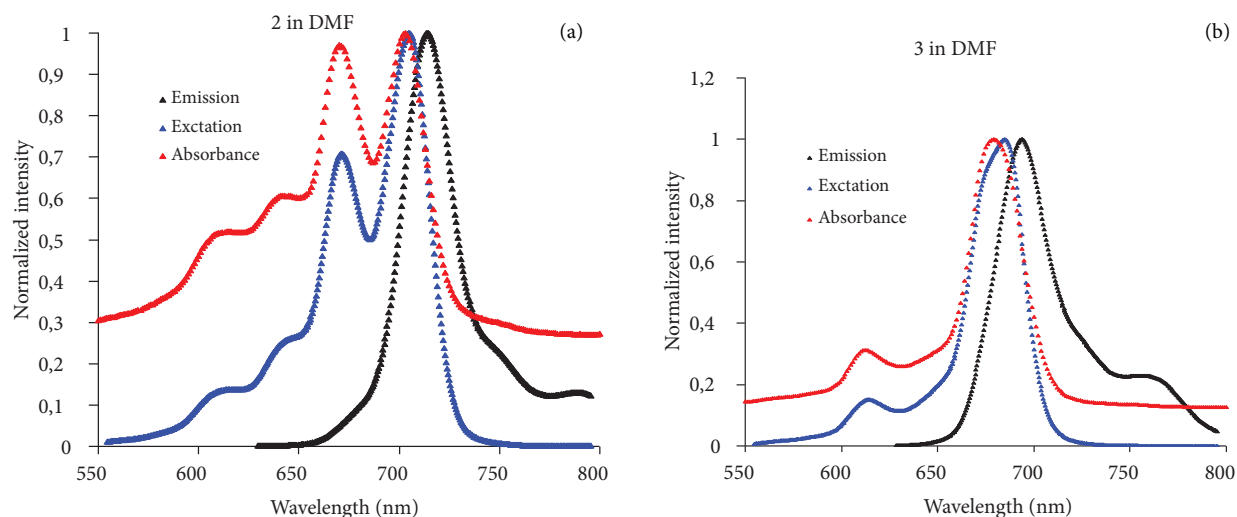


**Figure 4.** Absorption, excitation, and emission spectra for compounds **2** and **3**. Excitation wavelength = 615 nm in DMF.

### 2.3. Photophysical properties

The fluorescence quantum yields ( $\Phi_F$ ) of free base (**2**) and zinc (**3**) Pcs were studied in DMF. While the  $\Phi_F$  value of metal-free complex **2** ( $\Phi_F = 0.16$ ) is lower than characteristic of Pcs, the  $\Phi_F$  value of zinc Pc complex **3** ( $\Phi_F = 0.37$ ) is higher than characteristic of Pc complexes<sup>32</sup> and unsubstituted zinc Pc ( $\Phi_F = 0.30$ ) in DMF. Generally, the  $\Phi_F$  values of the Pcs that have different substituents are higher than those of standard zinc Pc. An increase in fluorescence intensity could occur with the presence of ligands, which decline the fluorescence quenching. Thus, the increase in the  $\Phi_F$  value for substituted Pc complexes in the presence of the ring substituents shows that the substituents quench the excited singlet state less, and therefore their fluorescence is more intense.

### 2.4. Photochemical properties

Singlet oxygen may be determined by 2 main methods: using chemical quenchers or using luminescence at 1270 nm. In this work, a singlet oxygen scavenger, 1,3-diphenylisobenzofuran (DPBF), a known quencher in organic solvents, was employed. Singlet oxygen quantum yield ( $\Phi_\Delta$ ) is a determination of singlet oxygen production and the  $\Phi_\Delta$  values were calculated via Eq. (3) in Section 3.3.3. Figure 5 shows spectral changes observed during photolysis of compound **3** in DMF in the presence of DPBF as an example. The reduction of DPBF

absorption was monitored using UV-Vis spectral changes. The Q band intensities for the compound were not changed during the  $\Phi_{\Delta}$  determinations, confirming that Pcs are not degraded through reactive singlet oxygen generation. The  $\Phi_{\Delta}$  values are 0.48 for compound **3** and 0.14 for compound **2** in DMF. The values of  $\Phi_{\Delta}$  were lower for the substituted complexes (**2** and **3**) when compared to unsubstituted zinc Pc ( $\Phi_{\Delta} = 0.56$ ) in DMF. The metal-free Pc complex has lower  $\Phi_{\Delta}$  values than the zinc Pc (**3**) due to metal effect.

Photodegradation study is a procedure whereby a Pc is degraded by light irradiation. The stabilities of studied Pc complexes (**2** and **3**) were determined in DMF solution by monitoring the decrease in the intensity of the Q band under irradiation with increasing time. Stable zinc Pc molecules show values as low as  $10^{-6}$  and, for unstable molecules, values of the order of  $10^{-3}$  have been reported. In the spectral changes observed for Pcs **2** and **3** during irradiation (see Figure 6 as an example for complex **2**), it was confirmed that photodegradation occurred without phototransformation. The photodegradation quantum yield of complex **2** is  $\Phi_d = 17.05 \times 10^{-4}$  and of complex **3** is  $9.12 \times 10^{-4}$ , and they are less stable when compared to unsubstituted zinc Pc ( $\Phi_d = 0.23 \times 10^{-4}$ )<sup>33</sup> in DMF.

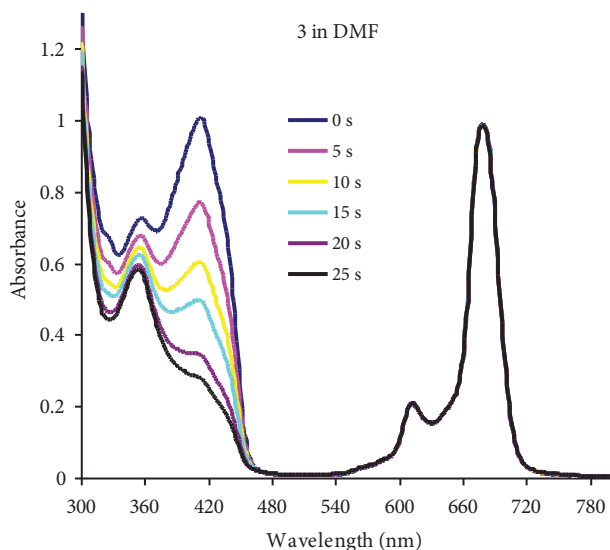


**Figure 5.** A typical spectrum for the determination of singlet oxygen quantum yield. This determination was for compound **3** in DMF at a concentration of  $1 \times 10^{-5}$  mol  $\text{dm}^{-3}$ .

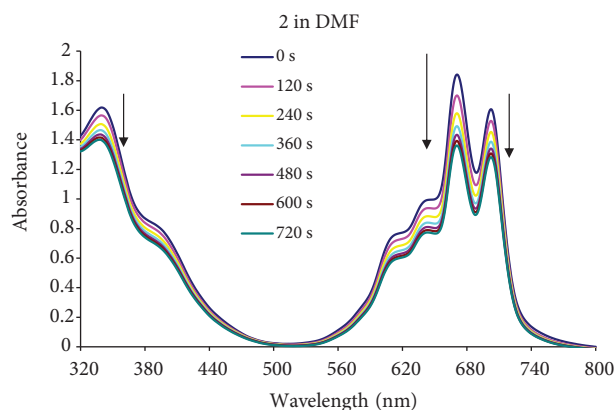


**Figure 6.** The photodegradation of compound **2** in DMF showing the disappearance of the Q band at 2-min intervals.

As a result, we explained the synthesis, characterization, and photophysical properties of tetrakis-(2,2-diphenylethoxy) Pcs in this work. The chemical structures of novel Pcs were confirmed by elemental analysis, as well as FT-IR, UV-Vis, mass, and  $^1\text{H}$  NMR spectroscopies. All studied Pcs (**2–5**) are very soluble in known organic solvents such as  $\text{CHCl}_3$ , DMF, DCM, toluene, THF, DMSO, and acetone. The effect that substituted Pcs have on the splitting of the Q band is highly influenced by the electronic properties of the substituent and the type of the central metal ion. The photophysical properties of synthesized Pcs **2** and **3** were determined in DMF in this work. To conclude, photophysical parameters of the Pcs studied together with their corresponding conjugates, especially complex **3**, show these molecules to be potential PDT agents.

### 3. Experimental

#### 3.1. Synthesis

##### 3.1.1. Synthesis of 4-(2,2-diphenylethoxy)phthalonitrile (1)

The mixture of 4-nitrophthalonitrile (0.50 g, 2.5 mmol) and 2,2-diphenylethanol (0.43 g, 2.5 mmol) was dissolved in dry dimethylformamide (20 mL) under N<sub>2</sub>. Finely anhydrous potassium carbonate (0.69 g, 5 mmol) was added in portions over 2 h. The reaction mixture was stirred at 45 °C for 48 h under N<sub>2</sub>. The solution was then poured into 200 mL of ice-water, and the precipitate was filtered off and washed several times with water. The final product was recrystallized from ethanol. Yield: 0.69 g (85%), mp: 121–122 °C. FT-IR (ATR):  $\nu_{\max}$ , cm<sup>-1</sup> 3081–3028 (CH, aromatic), 2970–2894 (CH, aliphatic), 2228 (C≡N), 1592 (C=C). <sup>1</sup>H NMR (400 MHz, CDCl<sub>3</sub>, 298 K):  $\delta$ , ppm 7.71 (d, 1H, aromatic), 7.36 (t, 4H, aromatic), 7.28 (t, 7H, aromatic), 7.19 (dd, 1H, aromatic), 4.56 (d, 2H, CH<sub>2</sub>), 1.59 (t, 1H, CH). Anal. Calc. for C<sub>22</sub>H<sub>16</sub>N<sub>2</sub>O: C, 81.46; H, 4.97; N, 8.64%. Found: C, 80.30; H, 4.71; N, 9.92%.

##### 3.1.2. Synthesis of 2,9(10),16(17),23(24)-tetrakis(2,2-diphenylethoxy) phthalocyanine (2)

A mixture of phthalonitrile derivative **1** (0.100 g, 0.3 mmol), a catalytic amount of 1.8-diazabicyclo[5.4.0]undec-7-ene (DBU), and amyl alcohol (4 mL) was heated and stirred at 160 °C for 20 h under N<sub>2</sub>. The obtained brown-green suspension was cooled to room temperature and the product was precipitated by the addition of the methanol. It was filtered off and dried in vacuo. Finally, pure phthalocyanine derivative was obtained by chromatography on silica gel via CHCl<sub>3</sub>/CH<sub>3</sub>OH mixture (90:10) as eluent. Yield: 0.04 g (40%). FT-IR (ATR):  $\nu_{\max}$ , cm<sup>-1</sup> 3290 (NH), 3085–3020 (CH, aromatic), 2920–2851 (CH, aliphatic), 1601 (C=C). UV-Vis (chloroform):  $\lambda_{\max}$  704, 668, 342 nm. <sup>1</sup>H NMR (400 MHz, CDCl<sub>3</sub>, 298 K):  $\delta$ , ppm 7.74–7.23 (br, 36H, aromatic), 4.67 (d, 8H, CH<sub>2</sub>), 1.75 (t, 4H, CH). MALDI-TOF MS: (m/z) 1300.7 [M+H]<sup>+</sup>. Anal. Calc. for C<sub>88</sub>H<sub>66</sub>N<sub>8</sub>O<sub>4</sub>: C, 81.33; H, 5.12; N, 8.62%. Found: C, 80.22; H, 4.90; N, 7.85%.

##### 3.1.3. General process for the syntheses of metallophthalocyanine derivatives (3–5)

A mixture of **1** (0.100 g, 0.3 mmol), anhydrous metal salt (0.073 mmol; 0.010 g ZnCl<sub>2</sub>, 0.009 g NiCl<sub>2</sub>, 0.009 g CoCl<sub>2</sub>), and a catalytic amount of 1.8-diazabicyclo[5.4.0]undec-7-ene (DBU) in amyl alcohol (4 mL) was refluxed under N<sub>2</sub> for 24 h. The final suspension was cooled to room temperature and the product was precipitated by the addition of methanol. It was filtered off and dried in vacuo. Finally, pure metallophthalocyanine derivatives were obtained by chromatography on silica gel via CHCl<sub>3</sub>/CH<sub>3</sub>OH mixture (90:10) as eluent. **3** (ZnPc): Yield: 0.05 g (51%). FT-IR:  $\nu_{\max}$ , cm<sup>-1</sup> 3087–3024 (CH, aromatic), 2916–2846 (CH, aliphatic), 1610 (C=C). UV-Vis (chloroform):  $\lambda_{\max}$  682, 350 nm. <sup>1</sup>H NMR (400 MHz, CDCl<sub>3</sub>, 298 K):  $\delta$ , ppm 7.73–7.07 (br, 36H, aromatic), 4.60 (d, 8H, CH<sub>2</sub>), 1.33 (t, 4H, CH). MALDI-TOF MS: (m/z) 1363.8 [M+H]<sup>+</sup>. Anal. Calc. for C<sub>88</sub>H<sub>64</sub>N<sub>8</sub>O<sub>4</sub>Zn: C, 77.55; H, 4.73; N, 8.22%. Found: C, 76.22; H, 5.02; N, 7.95%. **4** (NiPc): Yield: 0.06 g (62%). FT-IR:  $\nu_{\max}$ , cm<sup>-1</sup> 3054–3025 (CH, aromatic), 2958–2860 (CH, aliphatic), 1605 (C=C). UV-Vis (chloroform):  $\lambda_{\max}$  674, 330 nm. <sup>1</sup>H NMR (400 MHz, CDCl<sub>3</sub>, 298 K):  $\delta$ , ppm 7.34–7.20 (br, 36H, aromatic), 4.61 (d, 8H, CH<sub>2</sub>), 1.29 (t, 4H, CH). MALDI-TOF MS: (m/z) 1355.5 [M]<sup>+</sup>. Anal. Calc. for C<sub>88</sub>H<sub>64</sub>N<sub>8</sub>O<sub>4</sub>Ni: C, 77.93; H, 4.76; N, 8.26%. Found: C, 76.29; H, 4.90; N, 8.02%. **5** (CoPc): Yield: 0.05 g (55%). FT-IR:  $\nu_{\max}$ , cm<sup>-1</sup> 3075–3016 (CH, aromatic), 2965–2872 (CH, aliphatic), 1598 (C=C). UV-Vis (chloroform):  $\lambda_{\max}$

674, 326 nm. MALDI-TOF MS: (m/z) 1357.5 [M+H]<sup>+</sup>. Anal. Calc. for C<sub>88</sub>H<sub>64</sub>N<sub>8</sub>O<sub>4</sub>Co: C, 77.92; H, 4.76; N, 8.26%. Found: C, 76.30; H, 4.50; N, 7.98%.

### 3.2. Materials and instrumentation

FT-IR spectra were recorded on a PerkinElmer Spectrum One FT-IR (ATR sampling accessory) spectrophotometer. Elemental analyses were performed on a Thermo Flash EA 2000. <sup>1</sup>H NMR spectra were recorded on a Bruker Ultra Shield Plus 400 MHz spectrometer using TMS as an internal reference. Mass spectra were measured on a Bruker Microflex LT MALDI-TOF MS. Melting point was determined on an Electrothermal Gallenkamp apparatus. All reagents and solvents were of reagent grade and were obtained from commercial suppliers.

Absorption spectra in the UV-Vis region were recorded with a Shimadzu 2001 UV spectrophotometer. Fluorescence excitation and emission spectra were recorded on a Varian Eclipse spectrofluorometer using 1-cm path-length cuvettes at room temperature. Photoirradiation was done using a General Electric quartz line lamp (300 W). A 600-nm glass cut-off filter (Intor) and a water filter were used to filter off ultraviolet and infrared radiations, respectively. An interference filter (Intor, 700 nm with a band width of 40 nm) was additionally placed in the light path before the sample. Light intensities were measured with a POWER MAX 5100 (Molelectron Detector Inc.) power meter.

### 3.3. Photophysicochemical parameters

#### 3.3.1. Fluorescence spectra and quantum yields

Fluorescence quantum yields ( $\Phi_F$ ) were determined by the comparative method using Eq. (1):<sup>16</sup>

$$\Phi_F = \Phi_F(Std) \frac{F.AStd.n^2}{FStd.A.n_{Std}^2}, \quad (1)$$

where F and F<sub>Std</sub> are the areas under the fluorescence emission curves of the samples (**2** and **3**) and the standard, respectively. A and A<sub>Std</sub> are the respective absorbances of the samples and standard at the excitation wavelengths. n<sup>2</sup> and n<sub>Std</sub><sup>2</sup> are the refractive indices of solvents used for the sample and standard, respectively. ZnPc ( $\Phi_F = 0.30$  in DMF)<sup>34</sup> was used as the standard. Both the samples and standard were excited at the same wavelength.

#### 3.3.2. Singlet oxygen quantum yields

Singlet oxygen quantum yield ( $\Phi_\Delta$ ) determinations were performed as described in the literature.<sup>35,36</sup> Typically, a 3-mL portion of the phthalocyanine derivatives (absorbance:  $\sim 1.5$  at irradiation wavelength) containing the singlet oxygen quencher was irradiated in the Q band region with the photoirradiation set-up described in the literature.<sup>35,36</sup> Singlet oxygen quantum yields ( $\Phi_\Delta$ ) were determined in air using the relative method with ZnPc (in DMF) as a reference. DPBF was used as a chemical quencher for singlet oxygen in DMF. Eq. (2) was employed for the calculations:

$$\Phi_\Delta = \Phi_\Delta^{Std} \frac{R.I_{abs}^{Std}}{R^{Std}.I_{abs}}, \quad (2)$$

where  $\Phi_\Delta^{Std}$  is the singlet oxygen quantum yield for the standard ZnPc ( $\Phi_\Delta = 0.56$  in DMF<sup>37</sup>), and R and R<sub>Std</sub> are the DPBF photobleaching rates in the presence of the respective sample (**2** and **3**) and standard, respectively.

$I_{abs}$  and  $I_{abs}^{Std}$  are the rates of light absorption by the samples (**2** and **3**) and the standard, respectively. To avoid chain reactions induced by DPBF in the presence of singlet oxygen,<sup>38,39</sup> the concentration of the quencher (DPBF) was lowered to  $\sim 3 \times 10^{-5}$  mol dm<sup>-3</sup>. Solutions of sensitizer containing DPBF were prepared in the dark and irradiated in the Q band region using the set-up described above. DPBF degradation at 417 nm was monitored. The light intensity of  $7.05 \times 10^{15}$  photons s<sup>-1</sup> cm<sup>-2</sup> was used for  $\Phi_{\Delta}$  determinations.

### 3.3.3. Photodegradation quantum yields

Photodegradation quantum yield ( $\Phi_d$ ) determinations were performed as described in the literature.<sup>35,36</sup> Photodegradation quantum yields were determined using Eq. (3):

$$\Phi_d = \frac{(C_0 - C_t) \cdot V \cdot N_A}{I_{abs} \cdot S \cdot t}, \quad (3)$$

where  $C_0$  and  $C_t$  are the sample (**2** and **3**) concentrations respectively before and after irradiation,  $V$  is the reaction volume,  $N_A$  is the Avogadro constant,  $S$  is the irradiated cell area,  $t$  is the irradiation time, and  $I_{abs}$  is the overlap integral of the radiation source light intensity and the absorption of the samples (**2** and **3**). A light intensity of  $2.35 \times 10^{16}$  photons s<sup>-1</sup> cm<sup>-2</sup> was employed for  $\Phi_d$  determinations.

### Acknowledgment

The authors would like to thank Yıldız Technical University (Project No.: 2012-01-02KAP03).

### References

1. McKeown, N. B. *Phthalocyanine Materials: Synthesis, Structure and Function*; Cambridge University Press: Cambridge, UK, 1998.
2. Stuzhin, P. A. *J. Porphyrins Phthalocyan.* **1999**, *3*, 500–513.
3. Gregory, P. *J. Porphyrins Phthalocyan.* **2000**, *4*, 432–437.
4. Stuzhin, P. A.; Khelevina, O. G.; Angeoni, S.; Berezin, B. D. In *Phthalocyanines: Properties and Applications*; Leznoff, C. C.; Lever, A. B. P., Eds. VCH: New York, NY, USA, 1996.
5. Ozoemena, K.; Kutznetsova, N.; Nyokong, T. *J. Photochem. Photobiol. A* **2001**, *139*, 217–224.
6. Zimcik, P.; Miletin, M.; Ponec, J.; Kostka, M.; Fiedler, Z. *J. Photochem. Photobiol. A* **2003**, *155*, 127–131.
7. Seotsanyana-Mokhosi, I.; Nyokong, T. *J. Porphyrins Phthalocyan.* **2005**, *9*, 476–483.
8. Ogunsipe, A.; Maree, D.; Nyokong, T. *J. Mol. Struct.* **2003**, *650*, 131–140.
9. Yılmaz, Y.; Şener, M. K.; Erden, İ.; Avcıata, U. *Polyhedron* **2009**, *28*, 3419–3424.
10. Allen, C. M.; Sharman, W. M.; Van Lier, J. E. *J. Porphyrins Phthalocyan.* **2001**, *5*, 161–169.
11. Sehlotho, N.; Nyokong, T. *J. Mol. Catal. A* **2004**, *219*, 201–207.
12. Spiller, W.; Kliesch, H.; Wohrle, D.; Hackbarth, S.; Roder, B.; Schnurpfeil, G. *J. Porphyrins Phthalocyan.* **1998**, *2*, 145–158.
13. Bonnett, R. *Chem. Soc. Rev.* **1995**, *24*, 19–33.
14. Foley, S.; Jones, G.; Liuzzi, R.; McGarvey, D. J.; Perry, H. M.; Truscott, T. G. *J. Chem. Soc. Perkin Trans.* **1997**, *2*, 1725–1730.
15. Ion, R. M. *Curr. Topics Biophys.* **2000**, *24*, 21–34.

16. Maree, D.; Nyokong, T.; Suhling, K.; Philips, D. *J. Porphyrins Phthalocyan.* **2002**, *6*, 373–376.
17. Maree, S.; Phillips, D.; Nyokong, T. *J. Porphyrins Phthalocyan.* **2002**, *6*, 17–25.
18. Erdoğan, A.; Nyokong, T. *Dyes Pigm.* **2010**, *86*, 174–181.
19. Ogunsiye, A.; Nyokong, T. *J. Porphyrins Phthalocyan.* **2005**, *9*, 121–129.
20. Erdoğan, A.; Nyokong, T. *Polyhedron* **2009**, *28*, 2855–2862.
21. Seotsanyana-Mokhosi, I.; Chen, J. Y.; Nyokong, T. *J. Porphyrins Phthalocyan.* **2005**, *9*, 316–325.
22. Erdoğan, A.; Nyokong, T. *Inorg. Chim. Acta* **2009**, *362*, 4875–4883.
23. Spikes, J. D. *J. Photochem. Photobiol. A* **1986**, *43*, 691–699.
24. Ağırtaş, M. S. *Inorg. Chim. Acta* **2007**, *360*, 2499–2502.
25. Yılmaz, Y.; Mack, J.; Şener, K.; Sönmez, M.; Nyokong, T. *J. Photochem. Photobiol. A* **2014**, *277*, 102–110.
26. Kırbaç, E.; Yaşa Atmaca, G.; Erdoğan, A. *J. Organomet. Chem.* **2014**, *752*, 115–122.
27. Öztürk, C.; Erdoğan, A.; Durmuş, M.; Uğur, A. L.; Aytan Kılıçarslan, F.; Erden, İ. *Spectrochim Acta A* **2012**, *86*, 423–431.
28. Gouterman, M. In *The Porphyrins: Physical Chemistry, Part A*; Dolphin, D., Ed. Academic Press: New York, NY, USA, 1978.
29. Reddy, K. R. V.; Keshavayya, J. *Dyes Pigm.* **2002**, *53*, 187–194.
30. Ogunbayo, T. B.; Ogunsiye, A.; Nyokong, T. *Dyes Pigm.* **2009**, *82*, 422–426.
31. Bayrak, R.; Akçay, H. T.; Durmuş, M.; Değirmencioglu, I. *J. Organomet. Chem.* **2011**, *696*, 3807–3815.
32. Nyokong, T. *Coordination Chemistry Reviews* **2007**, *251*, 1707–1722.
33. Zorlu, Y.; Dumoulin, F.; Bouchu, D.; Ahsen, V.; Lafont, D. *Tetrahedron Lett.* **2010**, *51*, 6615–6618.
34. Khoza, P.; Antunes, E.; Nyokong, T. *Dyes Pigm.* **2014**, *104*, 57–66.
35. Seotsanyana-Mokhosi, I.; Kuznetsova, N.; Nyokong, T. *J. Photochem. Photobiol. A* **2001**, *140*, 215–222.
36. Ogunsiye, A. O.; Nyokong, T. *J. Mol. Struct.* **2004**, *689*, 89–97.
37. Spiller, W.; Kliesch, H.; Worchle, D.; Hackbarth, S.; Röder, B.; Schnurpfeil, G. *J. Porphyrins Phthalocyan.* **1998**, *2*, 145–158.
38. Erdoğan, A.; Nyokong, T. *J. Mol. Struct.* **2010**, *977*, 26–38.
39. Erdoğan, A.; Ogunsiye, A. O.; Nyokong, T. *J. Photochem. Photobiol. A* **2009**, *205*, 12–18.